

Intermittent subharmonic and chaos in parallel Buck converters with coupled interference signal

Lili Wang^{1,2*}, Junning Chen²

¹School of Electronic and Information Engineering, Anhui Jianzhu University, Hefei, Anhui Province, 230601, China

²School of Electronic and Information Engineering, Anhui University, Hefei, Anhui Province, 230601, China

*Corresponding author's e-mail:ll_wang@yeah.net

Abstract. This paper studies intermittent instabilities in parallel power system. Taking parallel buck converters with coupled interference signals as an example, model and actual system are established. By numerical simulation, the nonlinear behaviours are captured under some conditions. Characteristics and mechanism of intermittency are depicted by nonlinear theory. In this paper, mappings time to parameter are established and discrete iterative mappings for nonlinear systems are derived. All the simulation results are consistent with the theoretical analysis results. The research method adopted in the paper is applicable for the other parallel powersystems. The conclusion can provide a reference for the parallel converters to maintain stable operation and serves as a theoretical basis for further optimization design and system control.

1. Introduction

DC-DC converter is the core part of power supply. It is widely used in communication, instrumentation, household appliances and so on. It is a kind of nonlinear dynamical system [1]. In the past twenty years, some scholars have studied the nonlinear phenomenon in the converters. Many papers have found that lots of nonlinear phenomenon can be observed when converter works under the certain condition ^[2-4], which can be depicted by time series, bifurcation diagrams and etc.

Parallel converters are complex nonlinear systems. They are suitable for the needs of low voltage, large current and distributed modular power system and widely used in many fields. However, there are few reports about nonlinear behaviors in parallel converters because of close-loop structure and too many parameters. Motivated by the above discussions, this paper takes the parallel converter as the research object, establishes the mathematical model and simulation model of the system according to the working principle, observes practical operation by simulation and experiments and explores its mechanism by using nonlinear theory so as to provide effective reference for practical operation and circuit design.

2. Parallel Buck converters with coupled interference signal

2.1 Overview of system operation

As shown in figure 1, the system consists of two Buck converters connected in parallel.

D_1 and D_2 denote two diodes. S_1 and S_2 are switches. There are two operational amplifiers in the



system, they are marked as A . For converter 1, the error of the output voltage with the reference voltages is amplified by the voltage gain, and then it compares with the DC-offset voltage. So, a closed voltage feedback loop is formed to generate the control signal given by

$$v_{con1} = V_{offset} - K_{v1}(v - V_{ref}) \quad (1)$$

Where V_{offset} is DC offset voltage, K_{v1} is voltage gain of buck converter 1, v is capacitor voltage, it is one of the state variables for its continuity, V_{ref} is reference voltage.

For converter 2, the control voltage is obtained by adding an error current signal to the closed voltage feedback loop, which is given by

$$v_{con2} = V_{offset} - K_{v2}(v - V_{ref}) - K_i(i_2 - mi_1) \quad (2)$$

where K_{v2} is voltage gain of buck converter 2, i_1 is inductor current in converter 1, i_2 is inductor current in converter 2. As i_1 and i_2 cannot mutate, they are both state variables. K_i is current gain, and m is split ratio. The signal generator generates a saw tooth signal given by

$$v_{ramp} = V_L + (V_U - V_L)(t \bmod T) \quad (3)$$

where T is switching period. Within every period, the saw tooth signal increases linearly from V_L to V_U , where V_L is the lower limit voltage and V_U is the upper limit voltage.

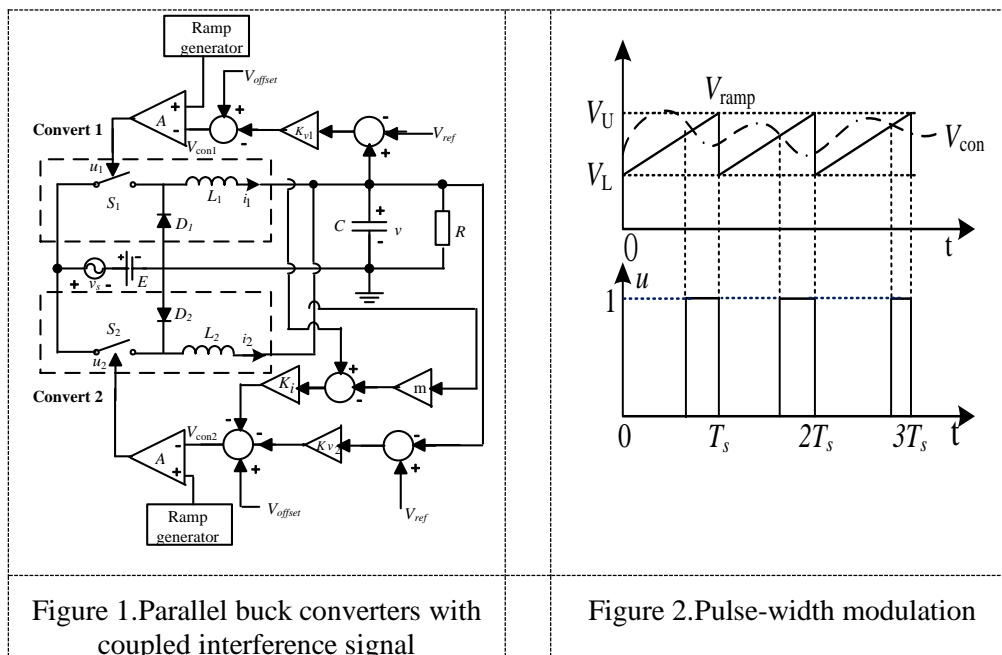


Figure 1. Parallel buck converters with coupled interference signal

Figure 2. Pulse-width modulation

The system adopts PWM (pulse-width modulation) mode^[5], the principle of modulation is described as follows: The control voltage is compared with the saw tooth voltage to form the pulse signal called as u . Then the pulse signal u^1 and u^2 drive the switch respectively. In this system, when the control voltage is lower than the saw tooth amplitude, the pulse signal outputs "1" and the switch is "on", otherwise the pulse signal outputs "0" and the switch is "off", as shown in Figure 2.

In practice, the system is often disturbed by external signals. Interference signals are transmitted or radiated into the circuit through the coupling channel^[6], which affects the normal operation of converters. For that, we introduce interference signals (the circuit is often interfered by such periodic sinusoidal signals in the RF environment) and add them to the input voltage,

$$E^* = E + v_s = E + \hat{v}_s \sin(2\pi f_0 t) = E[1 + \alpha_v \sin(2\pi f_0 t)] \quad (4)$$

where E is input voltage, \hat{v}_s is the voltage amplitude of the interference signal, f_0 is the frequency of interference signal. α_v is the amplitude ratio of the interference voltage to the input voltage, represents the intensity of the interference source, given by

$$\alpha_v = \hat{v}_s / E \quad (5)$$

Figure 1. shows parallel Buck converters with coupled interference signals. When each Buck converter works in CCM (Continuous Conduction Mode) [7], as the switching transistor and diode have two working states respectively, system may have four states during every circle. The state equation of each state is listed as follows:

$$\dot{x} = Ax + BE \quad (6)$$

where $x = [v \quad i_1 \quad i_2]^T$

$$A = \begin{bmatrix} -\frac{1}{(R+r_c)C} & \frac{R}{(R+r_c)C} & \frac{R}{(R+r_c)C} \\ -\frac{R}{(R+r_c)L_1} & -\frac{1}{L_1} \left(\frac{Rr_c}{R+r_c} + r_{L1} \right) & -\frac{1}{L_1} \left(\frac{Rr_c}{R+r_c} \right) \\ -\frac{R}{(R+r_c)L_2} & -\frac{1}{L_2} \left(\frac{Rr_c}{R+r_c} \right) & -\frac{1}{L_1} \left(\frac{Rr_c}{R+r_c} + r_{L2} \right) \end{bmatrix}, \quad B = \begin{bmatrix} 0 \\ \frac{u_1}{L_1} \\ \frac{u_2}{L_2} \end{bmatrix}$$

Where A and B are the coefficient matrices of converters.

2.2. Simulation results

According to the state equation, the simulation model is established by MATLAB, circuit parameters are chosen as follows:

Table 1 Component values.

Circuit Components	Value
Capacitor C , ESR r_c	$47\mu F, 0.01 \Omega$
Inductor L_1 , ESR r_{L1}	$20mH, 0.05\Omega$
DC offset voltage	$5V$
Input voltage E	$22V$
Current gain K_i	5
Lower limit voltage V_L	$3.8 V$
Switching period T	$400\mu S$
Load resistor R	10Ω
Inductor L_2 , ESR r_{L2}	$20mH, 0.2\Omega$
Reference voltage V_{ref}	$11.3V$
Voltage gain K_{v1}, K_{v2}	$3.5, 3.5$
Split ratio m	1
Upper limit voltage V_U	$8.2 V$

If the frequency of interference signal is n times of the switching frequency of the converters, n is a positive integer. Taking $n=1$ and $n=2$ as examples, the Poincare section of the system is observed and exhibited as figure 3(a) and (b). Poincare section describes the sample state at each switching point. It is a useful way to describe the operation of the system.

When $f_0 = f_s$ and $f_0 = 2f_s$, where f_0 is interference frequency, they are both characterized by only one intersection, showing the converters is in period-1, indicating that system is stable. If the frequency of interference signal is $1/n$ times of the switching frequency of the converters, Fig 3(c) and (d) show two examples with $n=2$ and $n=4$, parallel converters are in period-2 and period-4, characterized by 2 and 4 intersections on the Poincare sections.

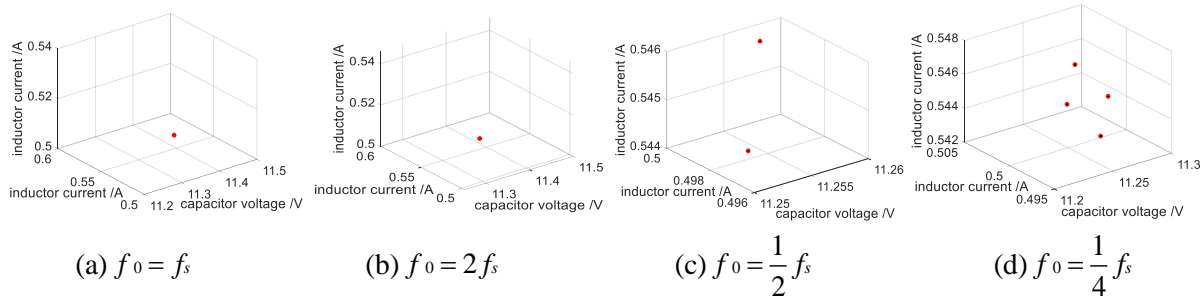


Figure 3. Poincaré section

However, in most case, the interference signal is random, and its frequency is not just the rational multiples of the switching frequency exactly. Generally, the frequency of the interference signal is close to the switching frequency. Therefore, assuming $f_0 = 2501\text{Hz}$, taking the interference intensity of intruding interference signal as the parameter. Figure 4. shows the time-bifurcation diagram of inductance current under different interference intensities.

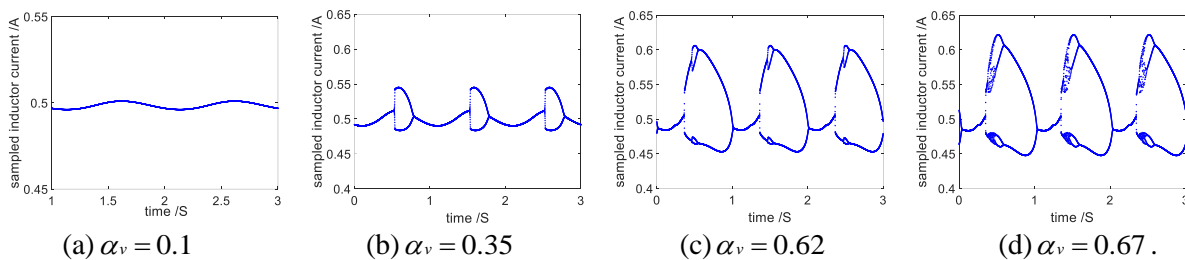


Figure 4. Time-bifurcation diagrams with varied intensity of the interference signal.

From these four figures, it can be observed as following:

1) When the interference signal intensity is weak, as shown in Figure 4. (a), the converters are still in period-1 although the sampled inductance current fluctuates around 0.5A, indicating that the interference signal has little impact on the converters.

2) As the intensity of the interference signal increases gradually, intermittency can be captured in the converters. The converter alternates between stable period- n and subharmonic states regularly. When $\alpha_v = 0.35$, converters experiences period-1 and period-2 subharmonic alternately, and when $\alpha_v = 0.62$ the converter experiences period-1 and period-2 subharmonic alternately. Figure. 4 (b) and (c) give the corresponding time-bifurcation diagrams.

3) Further increase the intensity of the coupling interference signal can cause the converter experiences period-1 and $2i$ subharmonic alternately. Until the intensity of the coupling interference signal reaches a critical value, intermittent chaos appears in converters, period 1 and chaos present alternately. Figure 4(d) gives the corresponding time bifurcation diagrams as $\alpha_v = 0.67$.

4) Intermittency is periodic. Intermittent period is defined as $T_{in} = 1/|f_0 - f_s|$ after summary and analysis. When the frequency of the interference signal is close to the switching frequency of the converter, converters take a long time to finish an intermittent process. In this example, there is 1Hz between two frequencies, so the intermittent period $T_{in} = 1\text{s}$.

3. Analysis of intermittency

The time - bifurcation diagram depicts the states varies with time. In order to analyze the stability of

parallel converters with different parameters, it is useful to describe the states by parameter-bifurcation diagrams. Therefore, it is necessary to establish the mapping relationship between time-bifurcation and parameter-bifurcation. The voltage of interference signal is transformed as follows:

$$v_s = v_s \sin(2\pi f_0 t) = E\alpha_v \sin(2\pi f_0 t) = E\alpha_v \sin[2\pi f_s t + 2\pi(f_0 - f_s)t] = E\alpha_v \sin(2\pi f_s t + \theta) \quad (7)$$

The interference signal after transformation can be regarded as the signal with the same frequency as the switching frequency of converters. θ is phase shift. The bifurcation diagram of the state variable as time varies over interval $[0,1]$ can be mapped to the diagram as phase shift varies over interval $[0,2\pi]$, as Figure 5. shown. The analysis of parameter bifurcation after mapping is equivalent to that of time bifurcation.

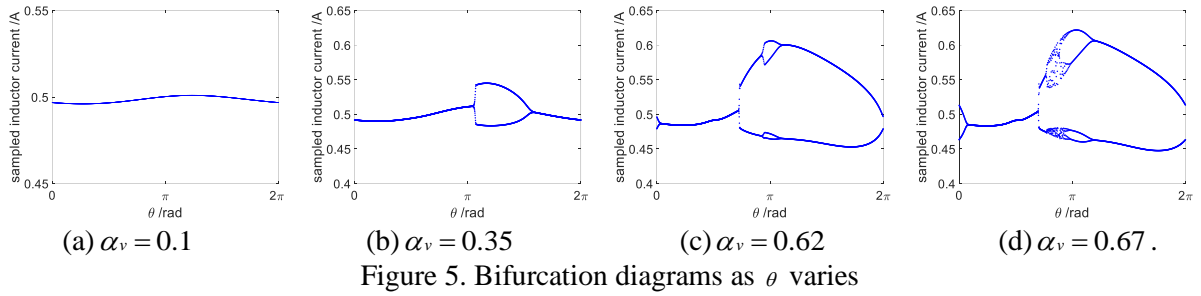


Figure 5. Bifurcation diagrams as θ varies

In order to study the stability of converters, we use nonlinear discrete time mapping based on the concept of discrete time model to analyze the nonlinear phenomenon of converters, that is, the state of converters is mapped from one sampling moment to the next sampling moment. This method has many advantages in using computer numerical calculation and reducing the amount of computation, and can successfully analyze various linear and nonlinear phenomena such as stable working state, bifurcation, quasi-period, chaos, and etc.

According to the circuit structure and working principle of parallel converters, if $d_1 < d_2$, where d_1 and d_2 are the duty circle values of two switches. Assuming the state variable at the beginning of the n th switching period is x_n , and the state variable at the beginning of the $n+1$ th switching period is x_{n+1} , then the discrete mapping of x_n to x_{n+1} can be expressed by following:

$$x_{n+1} = N(1-d_{2,n})N(d_{2,n}-d_{1,n})N(d_{1,n})x_n + N(1-d_{2,n})N(d_{2,n}-d_{1,n})M_1(d_{1,n})E[1+\alpha_v \sin(2\pi d_{1,n} + \theta)] + N(1-d_{2,n})M_3(d_{2,n}-d_{1,n})E[1+\alpha_v \sin(2\pi d_{2,n} + \theta)] + M_4(1-d_{2,n})E[1+\alpha_v \sin(2\pi + \theta)] \quad (8)$$

where $N_i(\xi) = e^{A_i \xi}$, $M_i = A_i [N_i - I] B_i$, $i=1,2,3,4$.

Switch function for switch 1 can be obtained by combining equations (1) and (3) as follows:

$$\begin{aligned} S_1(x_n, d_{1,n}) &= v_{con1} - v_{ramp1} \\ &= (V_{offset} + A_1 V_{ref}) + A_1^T [N(d_{1,n})x_n + (N(d_{1,n}) - I)A^{-1}B_1 E[1 + \alpha_v \sin(2\pi d_{1,n} + \theta)] - [V_L + (V_U - V_L)d_{1,n}]] \end{aligned} \quad (9)$$

where $A_1^T = (-A_1, 0, 0)$

Switch function for switch 2 can be obtained by combining equations (2) and (3) as follows:

$$\begin{aligned}
& S_2(x_n, d_{1,n}, d_{2,n}) \\
& = v_{con2} - v_{ramp2} = (V_{offset} + A_2 V_{ref}) + [A_2^T [N(d_{2,n})x_n + N(d_{2,n})A^{-1}B_1E[1 + \alpha_v \sin(2\pi d_{2,n} + \theta)]] \\
& + N(d_{2,n}T - d_{1,n}T)A^{-1}B_3E[1 + \alpha_v \sin(2\pi f_s t + \theta)] \\
& - N(d_{2,n} - d_{1,n})A^{-1}BE[1 + \alpha_v \sin(2\pi f_s t + \theta)] - A^{-1}B_3E[1 + \alpha_v \sin(2\pi d_{2,n} + \theta)] - [V_L + (V_U - V_L)d_{2,n}T]
\end{aligned} \tag{10}$$

where $A_2^T = (-A_2, mA_i, -A_i)$.

Duty cycle values d_1 and d_2 can be obtained by solving the equations $S_1(x_n, d_{1,n})=0$ and $S_2(x_n, d_{1,n}, d_{2,n})=0$.

Assuming the fixed point of the system is $X_Q = x_{n+1}$, the Jacobian matrix of the discrete iterative equation is shown as follows

$$J = \frac{\partial f}{\partial x_n} - \frac{\partial f}{\partial d_{1,n}} \left(\frac{\partial s_1}{\partial d_{1,n}} \right)^{-1} \frac{\partial s_1}{\partial x_n} - \frac{\partial f}{\partial d_{2,n}} \left(\frac{\partial s_2}{\partial d_{2,n}} \right)^{-1} \left[\frac{\partial s_2}{\partial x_n} - \frac{\partial s_2}{\partial d_{1,n}} \left(\frac{\partial s_1}{\partial d_{1,n}} \right)^{-1} \frac{\partial s_1}{\partial x_n} \right]_{x_n=x_Q} \tag{11}$$

Solving the equation of eigenvalues as below

$$\det[\lambda I - J(X_Q, d_{1Q}, d_{2Q})] = 0 \tag{12}$$

we get the trajectories of the eigenvalues as phase shift varies over interval [0,1] with different interference amplitudes as shown as Figure 6. From these figures, we have the following observations:

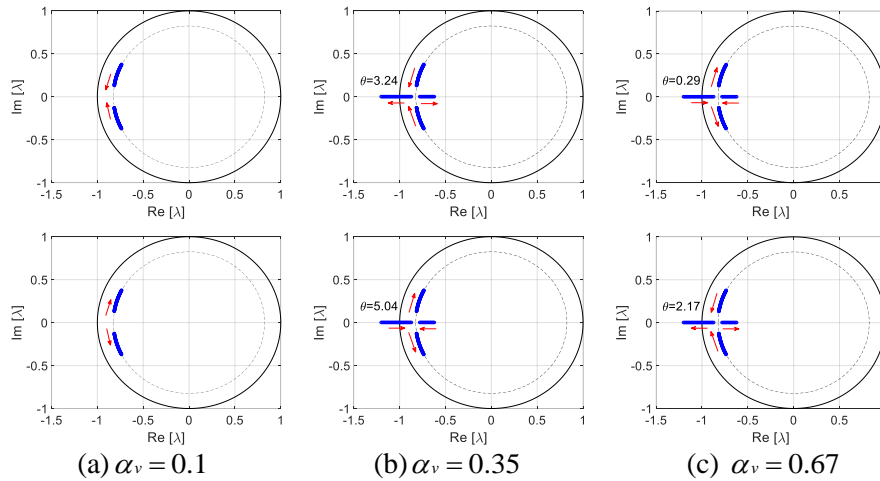


Figure 6. Loci of eigenvalues with varied amplitudes of the interference signal

1) When the intensity of interference signal is weak ($\alpha_v = 0.1$), eigenvalues move on the circle with a radius less than 1, and no matter how the phase shift changes, the eigenvalues are all in the unit circle, indicating converters are in the steady state, as shown in Figure. 6 (a).

2) As the intensity of interference signal increases ($\alpha_v = 0.35$), the eigenvalues move on the circle with a radius less than 1 toward the real axis. When θ increases up to 3.24, one eigenvalue leaves away the unit circle along the real axis, indicating the bifurcation occurs. With the increase of phase shift, eigenvalues move outside the unit circle along the real axis, until phase shift reaches to 5.04, and eigenvalues enters the unit circle again. Converters returns to the stable state. The trajectory of the eigenvalues vividly describes the complete intermittent subharmonics period. As shown as Figure.6(b), what the trajectory diagram describes is completely agrees with the information described in the previous time-bifurcation diagram shown as Figure.6(b).

3) For high intensity of interference signal ($\alpha_v = 0.67$), some eigenvalues move outside the unit circle. When θ increases up to 0.29, one eigenvalue on the real axis moves across the unit circle, converters changes from unstable to stable state. But when phase shift is 2.17, eigenvalues left the unit circle again. The converters lost stability again. As shown as Figure.6(c) the trajectory describes a complete intermittent chaos corresponds to the diagram as shown as Figure.6(c).

The results obtained by using the trajectory of the eigenvalue to analyze the state of the system are consistent with the results of the time-bifurcation diagrams and the parameter-bifurcation diagrams. Moreover, the boundary value of the system when the first instability occurs is exactly consistent with the previous simulation results. They prove the existence of intermittent instability in the system under the action of disturbance signal, and also show the correctness and effectiveness of mapping time bifurcation to parameter bifurcation.

4. Conclusions

In this paper, parallel Buck converters with coupled interference signal are constructed and investigated. We found that the intermittent instability of converters is characterized by intermittent harmonics or intermittent chaos. The research results show that when the system is disturbed by coupled parasitic signals, the intermittent harmonics and intermittent chaos can be captured. The specific mode of operation relates to the intensity of the interference. Coupling circuit conduction and radiation interference are the source of intermittency. The resonant parameter perturbation method can control the system in a stable state. The mapping of parameter-bifurcation and time-bifurcation proposed in the paper is effective and scientific for analyzing the stability of the system. The simulation results and experimental results are consistent with the analysis conclusion.

The conclusion can solve the troubles of engineers in practical work, and guide to design more stable and reliable converters. The numerical simulation, theoretical analysis and control methods adopted in this paper can also be extended to other systems in parallel.

Acknowledgments

This work was supported by the Key research projects of Natural Science in Universities in Anhui, Grant No. KJ2017A489 and No. KJ2015A031.

References

- [1] Subashini, M.(2017)Bifurcation and chaos in converter interfaces in solar PV systems-A review.Journal of Engineering Science and Technology Review,10:90-97.
- [2] Zhang, F.Y.,Hu,W.(2015) Chaos control and anti-control in Boost converter based on altering correlation. Acta Physica Sinica,64: DOI:10.7498/aps.64.048401
- [3] Harb, Ahmad M., Harb, Souhib M., Batarseh, Issa E.(2010) Chaos and bifurcation of voltage-mode-controlled buck dc-dc converter with multi control parameters.International Journal of Modelling and Simulation,30: 472-478.
- [4] Wang, L.B.,Meng, Z., Sun,Y.G.,(2017) Bifurcation and chaos analysis of power converter for switched reluctance motor drive. International Journal of Electronics.104: 157-173.
- [5] He, J., Zheng, X., Wang, W., Ren, Y.(2013) Terminal sliding mode control of Boost converter with chaos. Transactions of China Electrotechnical Society,28:104-108.
- [6] Li, G.L., Li, Chun Y.,Chen, X., Zhang, X.W.(2013) Chaos control of SEPIC converter based on resonant parametric perturbation method. Acta Physica Sinica,62: DOI: 10.7498/aps.62.210505
- [7] Jia, M.M., Zhang, G.S.(2016) Chaos control for the voltage-controlled buck converter. Journal of the University of Electronic Science and Technology of China,45:208-214.